Thermal-light-induced dynamics: Coherence and revivals in V-type and molecular Jaynes-Cummings systems

David Avisar* and A. D. Wilson-Gordon
Department of Chemistry, Bar-Ilan University, Ramat Gan 5290002, Israel
(Received 27 November 2015; published 24 March 2016)

We examine the interaction of thermal light with matter with emphasis on two aspects that have not been considered before. By employing a fully quantized Jaynes-Cummings–type interaction model on a V-type three-level system, we show that multimode thermal light induces coherence in the excited material states. This is in contrast to previous studies that suggest thermal light cannot induce coherence in material systems. We also show that the ratio between the field detuning and the interaction constant has a significant influence on the characteristic time-dependent dynamics. In particular, for some ratio regimes, the thermal light induces dynamics with a "coherentlike" collapse and revivals pattern rather than the familiar pattern. We then extend the Jaynes-Cummings model to a two-state Born-Oppenheimer potential energy surface molecular system where the internal vibrational degrees of freedom are fully taken into account. The matter-field bipartite system is represented, and propagated, in the full electronic bond-coordinate Fock product space. We show that single-mode thermal light induces extensive excited-state vibrational coherence in the molecule that, when observed in coordinate space, exhibits wave-packet-like dynamics. The molecular Jaynes-Cummings model we propose is useful for cavity molecular dynamics simulations.

DOI: 10.1103/PhysRevA.93.033843

I. INTRODUCTION

The Jaynes-Cummings (JC) model [1] is the fully quantum-mechanical formulation for the interaction of a two-level system with a single-mode radiation field. Its unique properties and extensions have been studied and reviewed for various configurations [2,3]. These include three-level matter systems, multiple-mode fields, multiple-photon interactions, and various initial conditions. New advances and applications have been recently reported in a special issue marking 50 years for the model (see, for example, [4–6]). Our interest in this work is the interaction of molecular systems with thermal light in a fully quantized framework. To achieve this, we present an extension of the JC model to molecular systems, represented in coordinate space, thereby including the molecular vibrational degrees of freedom.

The simplest model for a molecular system is perhaps the V-type three-level system. The interaction of three-level systems with quantized fields has been studied in a two-mode configuration, consisting mainly of pure states of the field, where neither of the modes induces both of the allowed transitions but only one particular transition [7–10]. Interestingly, these works considered populations and average-photon-number dynamics, but not coherence effect in the material system. The interaction of a quantized thermal field (which is a mixed state) with matter was studied for the first time soon after the JC model was introduced [11]. However, the material system considered there was a two-level system. Subsequent studies of matter interacting with a quantized thermal field have also focused on two-level systems [12–17]. It is expected, therefore, that analyzing the fully quantized interaction dynamics of a V-type three-level system with a thermal state of the field will be beneficial for understanding the interaction of molecular systems with thermal light.

The interaction of matter with thermal light is closely related to the ongoing efforts to study the sunlight-induced dynamics in natural photosynthetic systems. In particular, the question of whether these systems undergo coherent dynamics following excitation is under debate. Experimental studies have indicated the formation of vibrational and electronic coherence in photosynthetic systems excited, typically, by ultrashort laser pulses [18–25]. Theoretical studies have employed a number of approaches but have not yet reached a consistent conclusion regarding this question [26–32]. Typically, these studies consider a V-type level system as a model for the matter but do not consider the radiation dynamics, either because they employ a semiclassical formulation or trace over the field subspace prior to performing state propagation. Moreover, most of the theoretical approaches are approximate in some sense, as they involve semiclassical and perturbative formulations. Some of them rely on the presence of an intrinsic coupling between the material excited states, such as vacuum- or decay-induced coherence [31–33]. Others treat the material system following an assumed coherent excitation [34].

Knight and Radmore [12] have compared semiclassical and fully quantum-mechanical formulations for the thermal-light-induced dynamics in a two-level system. The results indicated different dynamics for the two formulations. Han *et al.* [35] have employed a semiclassical interaction model for studying the interaction of a more realistic molecular system with incoherent light, where the field is treated classically. The resultant dynamics indicate an irregular structure in coordinate space with fast decoherence. Since incoherent light is intrinsically statistical, the implementation of a semiclassical formulation for its interaction with matter requires the use of many separate realizations of the field; see also [36]. Field

*Author to whom correspondence should be addressed: david.avisar@gmail.com; Present address: Department of Applied Mathematics, Israel Institute for Biological Research, P.O. Box 19, 7410001, Ness-Ziona, Israel.

quantization, on the other hand, suggests a closed analytical expression for thermal states of the light, using the density matrix. Thus, it offers a convenient route for simulating the interaction of thermal light with a material system within a fully quantized framework, and in particular with a molecular system including its internal vibrational degrees of freedom. In light of this, our goal is to implement a fully quantized and exact (nonperturbative) formulation for the interaction of a Born-Oppenheimer molecular system with a (quantized) thermal state of the field.

In this study, we examine the interaction of multiple excited-state material systems with multimode thermal light using the density-matrix formalism. Specifically, we consider a V-type three-level system and extend the JC model to a molecular system of two-state Born-Oppenheimer potential energy surfaces (PESs). While the thermal light remains completely diagonal in Fock space during the interaction and does not induce coherence between the ground and excited state of the material subsystem, it does induce coherence between the material excited states, even when a multimode thermal field is used. In the molecular system, the excited-state coherence is manifested by wave-packet-like dynamics seen in the coordinate representation of the reduced density matrix of the material subsystem. We consider low and high initial average-photon-number regimes and different ratios between the field detuning and the interaction strength. In some regimes of high initial average photon number, thermal light shows "coherentlike" collapse and revival patterns rather than the characteristic "chaotic" or "random" pattern [12,37].

II. THEORETICAL FRAMEWORK

Conceptually, we treat the light-matter system as a bipartite composite system whose subsystems, the quantized material and field systems, interact via a JC-type interaction model. The dynamics are studied by propagating the density matrix of the composite system. We express the initial system by $\rho(0) = \rho_F(0) \otimes \rho_M(0)$ (where F and M stand for "field" and "material," respectively), and fully propagate it in time according to $\rho(t) = U(t)\rho(0)U^\dagger(t)$, where $U(t)$ is the system propagator that will be specified below. In practice, we apply this framework to a V-type three-level system interacting with one- and three-mode thermal states of the field. In addition, we apply it to a two-state Born-Oppenheimer molecular system interacting with a single-mode thermal state of the field. We now specify in detail the system Hamiltonians and the initial states we consider.

A. V system interacting with a multimode thermal state

The V-type three-level system is presented schematically in Fig. 1.

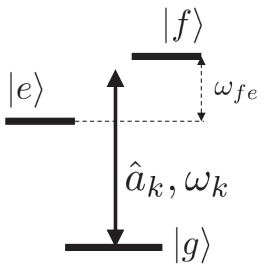

FIG. 1. V-type three-level scheme.

In our model, the JC-type Hamiltonian for this three-level system interacting with k modes of the radiation field is given in the material states basis by

$$H = \sum_i \omega_i |i\rangle\langle i| + \sum_k \omega_k \left(\hat{a}_k^\dagger \hat{a}_k + \frac{1}{2}\right) + \sum_k \sum_{i \neq g} \lambda_{i,k} (|i\rangle\langle g|\hat{a}_k + |g\rangle\langle i|\hat{a}_k^\dagger), \quad (1)$$

where we have invoked the dipole and rotating-wave approximations, and set $\hbar = 1$. The index $i = \{g,e,f\}$ stands for any of the material states, and ω_i denotes its energy. We denote the energy separation between the states by $\omega_{ij} = \omega_i - \omega_j$. The index k designates the kth mode of the field, and since we consider up to three modes, it takes the values 1,2, or 3. The operators $\hat{a}_k^\dagger$ and $\hat{a}_k$ are the photon creation and annihilation operators, respectively, corresponding to the kth mode, and operating on the photon states $\{|n_k\rangle\}$; ω_k is the mode frequency. Note that $\{|n_k\rangle\}$ denotes the photon states corresponding to the kth-mode Fock space. We define the field detuning with respect to ω_i by $\Delta_{i,k} = \omega_i - \omega_k$. The parameter $\lambda_{i,k}$ is the matter-field interaction constant for the coupling of the states $|g\rangle$ with either of the excited states, $|e\rangle$ ($\lambda_{e,k}$) or $|f\rangle$ ($\lambda_{f,k}$), through the kth mode. Note that each of the modes is allowed to couple the ground state with any of the excited states, and also that this model excludes any intrinsic coupling between the excited states. For simplicity, in the single-mode case we omit the index k from the parameters defined above.

For the interaction dynamics we consider here, the material system is initially in its ground state $\rho_M(0) = |g\rangle\langle g|$. The initial state of the field is either a thermal state or a coherent state. A single-mode thermal state of index k takes the form $\rho_{F,k}(0) = \sum_{n_k} p_{n_k} |n_k\rangle\langle n_k|$, with $p_{n_k} = \frac{\bar{n}_k^{n_k}}{(1+\bar{n}_k)^{n_k+1}}$, and the average photon number $\bar{n}_k$ is given by the Boltzmann distribution [37]. For a single-mode coherent state $|\alpha_k\rangle$ with index k, $|\alpha_k\rangle = e^{-\frac{1}{2}|\alpha_k|^2} \sum_{n_k} \frac{\alpha_k^n}{\sqrt{n_k!}} |n_k\rangle$, where $|\alpha_k|^2 = \bar{n}_k$ is the average field photon number. The corresponding density matrix is $\rho_{F,k}(0) = |\alpha_k\rangle\langle\alpha_k|$. The initial state of a multimode field is a tensor product of the individual single-mode states, $\rho_F(0) = \bigotimes_k \rho_{F,k}(0)$. The initial state of the composite system is $\rho(0) = \rho_F(0) \otimes \rho_M(0)$, and the state of the system at any time in its evolution is given, explicitly, by

$$\rho(t + dt) = e^{-iHdt} \rho(t) e^{iHdt}. \quad (2)$$

The state of each subsystem is obtained by tracing $\rho(t)$ over the space of the other subsystem (or over the spaces of the other subsystems, in the general case of multimode), that is,

$$\rho_A(t) = \mathrm{Tr}_B[\rho(t)]. \quad (3)$$

Finally, since we are interested in the excited-state coherence, we shall use the function $\mathrm{C}(t)$ (defined below) as a measure of coherence between the excited states,

$$\mathrm{C}(t) = \frac{|\rho_{M,fe}(t)|^2}{\rho_{M,ee}(t)\rho_{M,ff}(t)}. \quad (4)$$

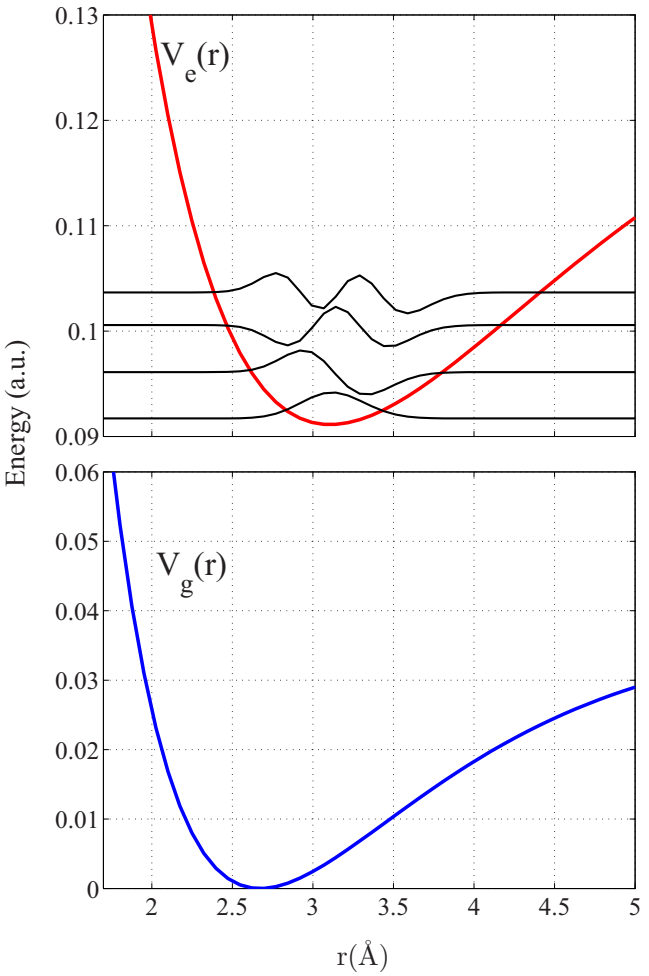

FIG. 2. Ground (bottom panel, blue) and excited (upper panel, red) Born-Oppenheimer potential energy surfaces of a diatomic molecular system. In the excited state we show the first four vibrational eigenstates with offset energies.

B. Two-state Born-Oppenheimer system interacting with a single-mode thermal state

We extend the JC model and formulate the interaction of a quantized field with a two-state Born-Oppenheimer PES (molecular) system, where, as specified below, the molecular vibrational degrees of freedom—that is, nuclei separations—are taken into account. In Fig. 2 we show the ground (blue) and excited (red) state PESs of a diatomic molecular system which we use in our simulations in this work. In the excited state, the first four vibrational eigenstates are also shown (with offset energy scale).

The field is represented in Fock space, and the molecular system is spanned by the two-dimensional electronic space and the continuous coordinate space for the nuclei separation. We denote the Hamiltonian of the interacting matter and field systems by $H_{\rm mol}$, whose explicit form in the two-dimensional electronic states basis is

$$H_{\rm mol} = \sum_{i=g,e} H_i(\boldsymbol{r})|i\rangle\langle i| + \omega\left(\hat{a}^\dagger\hat{a} + \frac{1}{2}\right) + \lambda(|e\rangle\langle g|\hat{a} + |g\rangle\langle e|\hat{a}^\dagger), \quad (5)$$

where $H_i(\boldsymbol{r}) = V_i(\boldsymbol{r}) + T$ is the nuclear Hamiltonian of the ith molecular electronic state (ground $|g\rangle$ and excited $|e\rangle$), with the PES $V_i(\boldsymbol{r})$ and the kinetic energy operator $T = -\frac{1}{2\mu}\nabla^2$. The parameter μ is the molecular reduced mass. Note that we have omitted the mode index k, since we consider only a single-mode field. We denote the (vibrational) eigenstates of $H_i(\boldsymbol{r})$ by $\psi_{i,\nu}(\boldsymbol{r})$, where ν is the vibrational quantum number. In writing the Hamiltonian of Eq. (5) we invoke the dipole, Condon, and rotating-wave approximations.

We examine the dynamics of the molecular system interacting with either a single-mode thermal or coherent state of the field, whose initial state is $\rho_F(0)$, as specified above. The initial molecular (ground) state is $\rho_M(0) = |g,\psi_{g,0}\rangle\langle g,\psi_{g,0}|$. The initial state of the system is the tensor product of the initial states of the two subsystems, and its state at any time in the course of interaction is

$$\rho(t+dt) = e^{-iH_{\rm mol}dt}\rho(t)e^{iH_{\rm mol}dt}. \quad (6)$$

The density matrix is represented and propagated in the electronic $\otimes$ bond-coordinate $\otimes$ photon-Fock product space. It is convenient to employ the "split operator" method [38] for the propagation and separate the kinetic energy term of the Hamiltonian from the rest of the terms. Thus, for each time step the propagator is $e^{-iH_{\rm mol}dt} \approx e^{-iTdt}e^{-i\tilde{H}_{\rm mol}dt}$, where $\tilde{H}_{\rm mol}$ is the full molecular Hamiltonian of Eq. (5) with the operator T excluded.

III. RESULTS AND DISCUSSION

A. V-type system interacting with single-mode thermal field

In this section, we consider the interaction of a V-type three-level system with single-mode thermal light. The energy of the excited state $|e\rangle$ is $\omega_e = 0.0911$ a.u., relative to the ground state, and the excited-state separation is $\omega_{fe} = 1.14 \times 10^{-3}$a.u. This separation corresponds to 250 cm^{-1}, which is a realistic vibrational level spacing in a molecule. The two latter parameters are kept fixed for the V-system cases considered in this work. The other parameter values used are specified below for each case that we consider. Note that all the parameter values given below are in atomic units unless specified otherwise. We shall consider a number of cases that differ in the field initial average photon number $\bar{n}$ and in the ratio $\frac{\Delta_i}{\lambda_i}$.

In the Appendix, we derive the analytical expressions for the material populations and coherence for the V system interacting with the single-mode thermal state of the field where the field frequency is tuned in the middle of the excited-state spacing, and the interaction constants are set equal. We use these analytical expressions to interpret some of the results presented in our work.

1. Case I: $\bar{n} \ll 1$ and $\frac{\Delta_i}{\lambda_i} > 1$

Our interest in the low-$\bar{n}$ regime stems from the fact that the average photon number characteristic of sunlight is 10^{-2} [37]. In case I, we consider a V system interacting with a single-mode thermal state initially with $\bar{n} = 0.008$ (corresponds to temperature of 6000 K at wavelength of 495.9 nm), detuning of $\Delta_e = 7.59 \times 10^{-4}$, and the interaction constants $\lambda_e = 1.5 \times 10^{-4}$ and $\lambda_f = 10^{-4}$. The initial state of

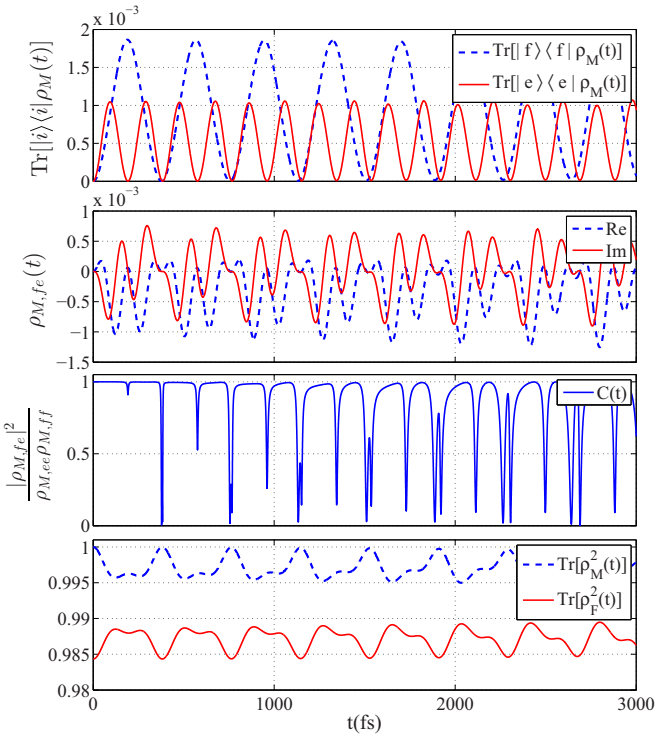

FIG. 3. From top to bottom: Excited-state populations ($|f\rangle$ state: blue dashed line; $|e\rangle$ state: red solid line), coherence element (real: blue dashed line; imaginary: red solid line), coherence measure, and partial traces (material: blue dashed line; field: red solid line) obtained for the V system interacting with a single-mode thermal state, initially with $\bar{n} = 0.008$ and $\frac{\Delta_i}{\lambda_i} > 1$.

the light is constructed with the first 11 Fock states such that the trace of the density matrix numerically converges to 1. The field frequency is detuned from both the excited states, as can be expected for a molecular system with many excited-state vibrational levels.

In Fig. 3, we show some of the dynamical measures obtained for this configuration. From top to bottom, we show the material excited-state populations $\mathrm{Tr}[|i\rangle\langle i|\rho_M(t)]$, the real and imaginary parts of the material excited-state coherence element $\rho_{M,fe}(t)$, the measure of excited-state coherence $\mathrm{C}(t)$, and at the bottom the traces of the material and field squared reduced density matrices $\mathrm{Tr}[\rho_M^2(t)]$ and $\mathrm{Tr}[\rho_F^2(t)]$. For the interaction of the same V system with a coherent state of the light of the same initial average photon number, the dynamical patterns (not shown) are indistinguishable from these shown in Fig. 3. The only difference is that $\mathrm{Tr}[\rho_{M,F}^2(t)] = 1$ since the states are pure.

The periods recognized for the populations correspond to the actual detunings, that is, Δ_e and Δ_f. This is understood by inspecting Eq. (A12), where the oscillatory term is governed by the detuning. The excited-state material coherence element $\rho_{M,fe}$ reveals also a higher-frequency component (of about 134 fs) which corresponds to the state separation ω_{fe}; this is evident in Eq. (A13) in the Appendix by the double-detuning frequency component. In addition to the coherence element, we show $\mathrm{C}(t)$ as a measure for the excited-state coherence. The excited-state subspace coherence is maximal as this measure approaches 1. It is reduced when the coherence element is minimal. The material populations, excited-state coherences, and coherence measures in Fig. 3 and its coherent-state analog (not shown) are indistinguishable. This result is reminiscent of that obtained when comparing the interaction of single-mode thermal and coherent states, initially with $\bar{n} = 1$, with an excited two-level system by Cummings [11], whose physical meaning was considered "obscure." By considering the analytical dynamical expressions in the Appendix for the case of a single-mode coherent state, it is evident that the high degree of similarity between the thermal and coherent cases is a direct consequence of the similar photon-number statistics of the two fields for the $\bar{n} \ll 1$ regime we consider here. On the other hand, $\mathrm{Tr}[\rho_M^2(t)]$ and $\mathrm{Tr}[\rho_F^2(t)]$ show different behavior for the two field cases. In the mixed-field-state scenario (interaction with the thermal light), both traces are generally < 1 and thus indicate the subsystems are not pure but mixed states. In addition, they oscillate out-of-phase as if purity is exchanged between the subsystems. On the other hand, as mentioned above, in the pure scenario (interaction with the coherent state) both traces equal 1, as is well known for a pure system.

Throughout the interaction of the thermal light with the V system, $\rho_F(t)$ remains diagonal in Fock space (which is easily verified by the analytical derivation in the Appendix); in other words, no coherence is generated in the thermal field. This is a direct physical consequence of the fact that the field is initially diagonal and from the nature of the interaction, as we shall explain shortly. From the material coherence perspective, it means that the thermal state does not induce coherence between the material ground and excited states (verified by the analytical derivation in the Appendix). The coherent state, on the other hand, induces coherence between the material ground and excited states. This distinction between the thermal and coherent states (along with the difference of the traces, mentioned above) indicates that the two types of field states are basically different, although the material populations and coherences are similar.

The reason for the absence (presence) of coherence between the material ground and excited states for the thermal (coherent) state is the following. According to our model, the interaction of a single Fock state, say $|n\rangle$, with the material ground state $|g\rangle$ produces the general superposition $a|g,n\rangle + (b|e\rangle + c|f\rangle)|n-1\rangle$, which in the material subspace (that is, after tracing over the field space) corresponds to a mixed state of the material ground and excited states. On the other hand, the superposition between the excited states is a source of coherence. Thermal light is a statistical mixture of single Fock states and, therefore, may induce only excited-state coherence in the material subsystem. Note that the absence of coherence between the ground and excited states is related to the vanishing of the material dipole-moment in this scenario, as pointed out in [15] for a two-level system. In contrast, since a coherent state is a *coherent* superposition of neighboring Fock states, its interaction with the material ground state will generate coherence between the material ground and excited states (since they share common photon states), and also among the excited states themselves. In this context, a Schrödinger cat (coherent) state [37] is expected to behave just like a thermal state, as already noted elsewhere [39],

although it is a pure state. The explanation given above for the thermal state applies in this case as well. To the best of our knowledge, the excited-state coherence of such a material system, induced by thermal light, has never been examined before. It is obtained in the model presented here through an exact quantum-mechanical treatment without any intrinsic coupling between the excited states. Such couplings were introduced in a number of previous studies [31–33] and were necessary to allow the material excited-state coherence.

Although we do not show it here, for a $\frac{\Delta_i}{\lambda_i} < 1$ regime (with $\bar{n} \ll 1$), the thermal- and coherent-induced dynamics also show almost identical patterns, with periods dictated by the interaction constant values (as is familiar for resonant case dynamics, and is easily verified using the analytical expressions given in the Appendix).

In light of the (partial) similarity in the material subsystem dynamics induced by the thermal and coherent states, the question may be raised concerning whether this behavior is expected or not. Although the similar photon statistics of the thermal and coherent states with $\bar{n} \ll 1$ gives a satisfactory explanation, this question may perhaps be strengthened by claiming that a single-mode thermal state is first-order coherent. It is well known that a coherent state is coherent in the general sense (that is, to any degree of coherence) [40]. Indeed, a single-mode thermal state is first-order coherent [40], regardless of its average photon number $\bar{n}$. Therefore, if single-mode thermal and coherent states induce similar dynamics because both are first-order coherent, then both states of the light are expected to induce similar dynamics regardless of their initial average photon number. Moreover, although a single-mode thermal state is first-order coherent, it is not second-order coherent [40], and thus it is not coherent (in the general sense), and differs, basically, from the coherent state (as we have actually shown above for the case of $\bar{n} = 0.008$). Last, a multimode thermal state is not even first-order coherent [40]. Hence, to establish a more general characteristic of thermal light interacting with matter, it would be desirable to examine the interaction of a V system with a single-mode thermal light of high average photon number and with multimode thermal light.

2. *Case II:* $\bar{n} \gg 1$ *and* $\frac{\Delta_i}{\lambda_i} \ll 1$

For the high-average-photon-number regime we use $\bar{n} = 10$. In this case, the dynamic patterns are complex and strongly depend on the ratio $\frac{\Delta_i}{\lambda_i}$. We first consider the small-ratio regime with $\lambda_e = 0.01$, $\lambda_f = 0.02$, and $\Delta_f = 3.80 \times 10^{-4}$. The number of Fock states used for the $\bar{n} = 10$ case is 120.

In Fig. 4 we show the time dependence of the populations (top panel), excited-state coherence element (middle panel), and the coherence measure C(t) (bottom panel) for the V system interacting with the single-mode thermal state and the specified $\frac{\Delta_i}{\lambda_i}$ ratio. (The time dependence of the average photon number, not shown, follows that of the ground-state population.)

Apparently, the induced dynamics follows the "chaotic" structure, which is characteristic of a thermal mode, of high enough $\bar{n}$, interacting resonantly with, for example, a two-level system [12,37]. As with the $\bar{n} \ll 1$ case, the reduced field density matrix (not shown) remains completely diagonal and

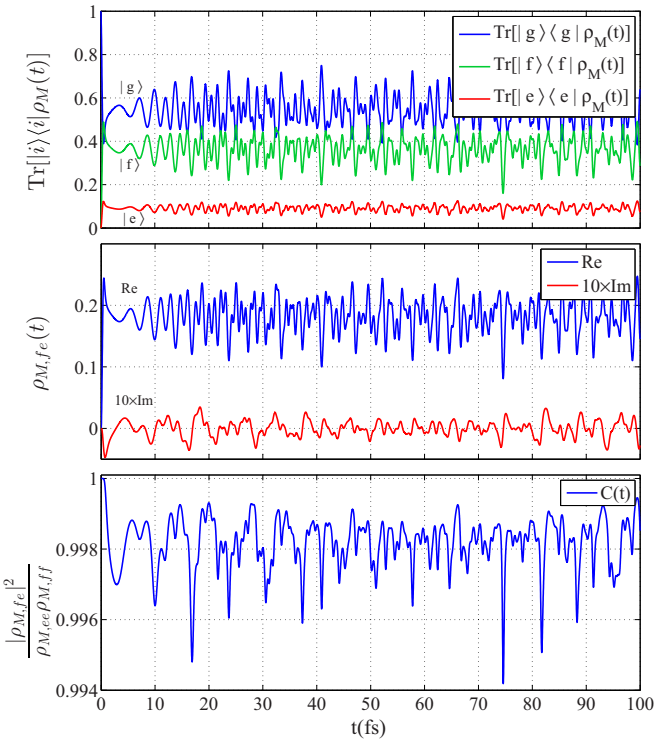

FIG. 4. From top to bottom: populations, excited-state coherence, and coherence measure, obtained for the V system interacting with single-mode thermal state, initially with $\bar{n} = 10$ and $\frac{\Delta_i}{\lambda_i} \ll 1$. Note the interpretation next to the line.

no coherence is induced between the ground and excited states; the interaction mechanism stays the same. In addition, $\mathrm{Tr}[\rho_M^2(t)]$ and $\mathrm{Tr}[\rho_F^2(t)]$ (not shown) are both < 1, thus indicating that the states are not pure. Although we do not show it here, the same interaction configuration with a coherent state shows the collapse and revival pattern characteristic of a coherent state [3,37]. In contrast to the low-$\bar{n}$ regime, in the current case the thermal and coherent state induce completely different time-dependent dynamics. As far as excited-state coherence is concerned, it is clear from Fig. 4 that, first, it is induced by the thermal state, and second, it follows a chaotic time dependence as well, and persists with steady intensity. The excited-state coherence measure indicates that a high degree of coherence persists throughout the interaction. These simulation results are easily verified using the analytical dynamical expressions given in the Appendix.

In this context, it is relevant to mention previous studies that have employed semiclassical formulations for the interaction of thermal light with matter. As mentioned above, Knight and Radmore [12] have compared fully quantized and semiclassical formulations for the interaction of thermal light with a two-level system and reported different dynamical patterns for the two. In addition, Jiang and Brumer [27] have also examined semiclassical perturbative formulation for the interaction of thermal light with a multilevel structureless material system. They concluded that no coherence between the material energy states is expected. The creation of a mixed state was also predicted by employing the von Neumann equation for the interaction of a V system with classical partially incoherent

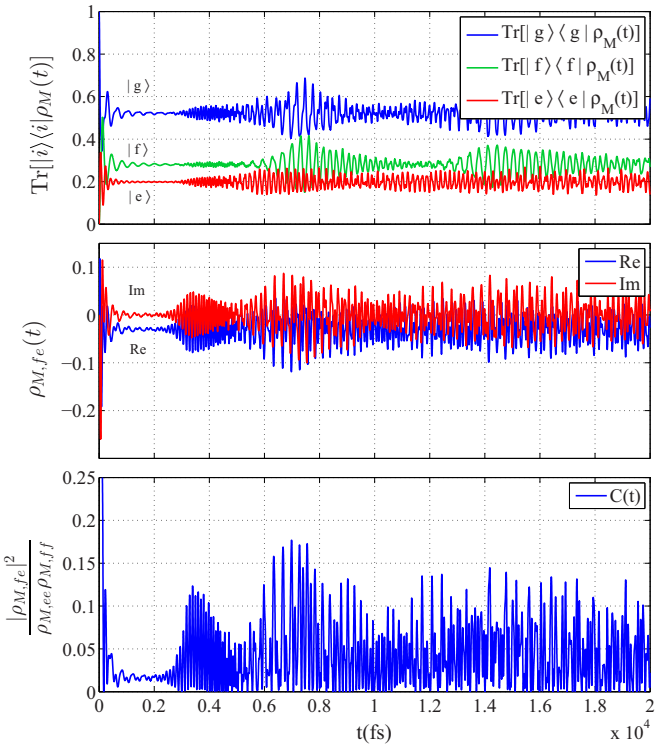

FIG. 5. From top to bottom: populations, excited-state coherence element, and coherence measure obtained for the V system interacting with single-mode thermal state, initially of $\bar{n} = 10$ and $\frac{\Delta_e}{\lambda_e} \approx 5$, $\frac{\Delta_f}{\lambda_f} \approx 4$. Note the interpretation next to the line.

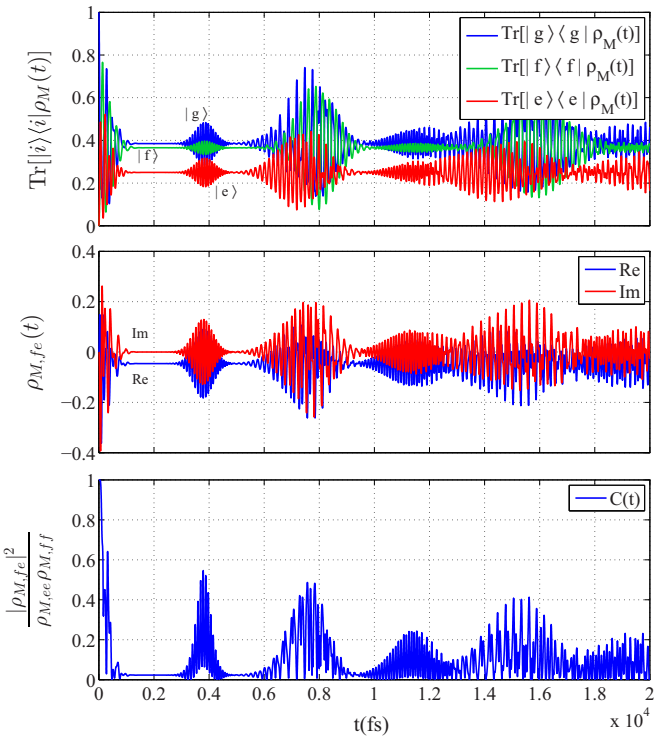

FIG. 6. From top to bottom: populations, excited-state coherence element, and coherence measure obtained for the V system interacting with a single-mode coherent state, initially with $\bar{n} = 10$ and $\frac{\Delta_e}{\lambda_e} \approx 5$, $\frac{\Delta_f}{\lambda_f} \approx 4$. Note the interpretation next to the line.

light [36]. The results we present above, both for low and high average photon numbers, contradict this conclusion (and those of subsequent studies, as is shown below). A thorough semiclassical study of the interaction of thermal light with matter may therefore be of interest for a full understanding of its comparison with the fully quantized model.

3. *Case III: $\bar{n} \gg 1$ and $\frac{\Delta_i}{\lambda_i} > 1$*

We consider now the case of relatively high field detuning. In Fig. 5, we show the populations, excited-state coherence, and coherence measure (top, middle, and bottom panels, respectively) of the V system interacting with a single-mode thermal light with initially $\bar{n} = 10$, interaction constants $\lambda_e = 1.5 \times 10^{-4}$ and $\lambda_f = 10^{-4}$, and detuning $\Delta_f = 3.80 \times 10^{-4}$. In Fig. 6 we show the same dynamical measures for a similar system, but the field is initially a coherent state.

Apparently, the thermal light induces dynamics with an unusual collapse-and-revivals pattern, which is far from the characteristic chaotic structure of thermal light. The collapse-and-revivals structure is more reminiscent of a coherent-state-induced dynamics and seems to present distinct frequency components. Inspecting the populations and coherence element time dependence reveals that during different periods of times the dynamics is governed by different frequency components. Specifically, at some periods the dynamics is governed by the detuning while at others, by the interaction constant, or the excited-state spacing for the coherence. As the ratio $\frac{\Delta_i}{\lambda_i}$ increases, an even more distinct time dependence of the collapse-and-revivals pattern is obtained, as exemplified in Fig. 7 for the thermal state with initially $\bar{n} = 10$ and $\lambda_e = 3 \times 10^{-5}$ and $\lambda_f = 5 \times 10^{-5}$. The three examples shown for the actual case present a structured pattern for the function $C(t)$ that persists throughout the interaction dynamics with varying intensity. Its detailed dynamical analysis remains beyond the scope of the current work. We should note here as well that for the thermal-light-induced dynamics, $\mathrm{Tr}[\rho_M^2(t)]$ and $\mathrm{Tr}[\rho_F^2(t)]$ (not shown) are both < 1, which indicates that the states are not pure.

In fact, depending on the particular values, the $\frac{\Delta_i}{\lambda_i} > 1$ case for a thermal light interacting with the V system shows a wealth of dynamical structures, which we do not consider here in detail. By inspecting and analyzing the analytical expressions of Eqs. (A14) and (A15) in the Appendix, it is clear that the dynamics shows a nontrivial dependence on both the detuning and interaction constant—it is not only the ratio $\frac{\Delta_i}{\lambda i}$ that determines which term dominates within the generalized Rabi frequency, see the generalized Rabi frequency for the case derived in the Appendix $\Omega_n \equiv \Delta^2 + 2\lambda^2 n$, but also the actual photon-state quantum number n. As a result, the term $\lambda^2 n$ may dominate although $\Delta > \lambda$, and the summation over the photon quantum number should include both detuning and interaction constant components. The resulting dynamical expressions thus superpose frequency components of both the detuning and the interaction constants. A detailed analysis of the relevant various cases is beyond the scope of this work but can be constructed based on the analytical derivation we present in the Appendix.

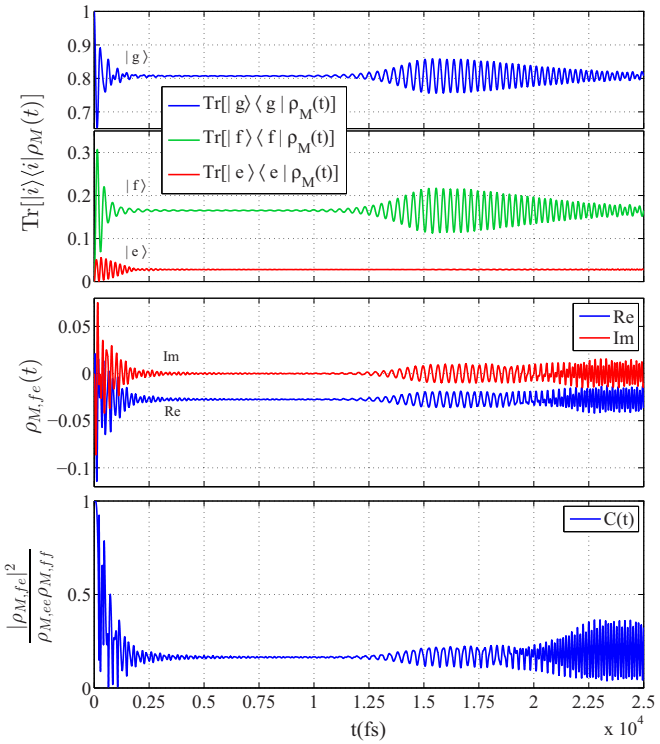

FIG. 7. From top to bottom: populations, excited-state coherence element, and coherence measure obtained for the V system interacting with a single-mode thermal state, initially with $\bar{n} = 10$ and $\frac{\Delta_e}{\lambda_e} \approx 25$, $\frac{\Delta_f}{\lambda_f} \approx 8$. Note the interpretation next to the line.

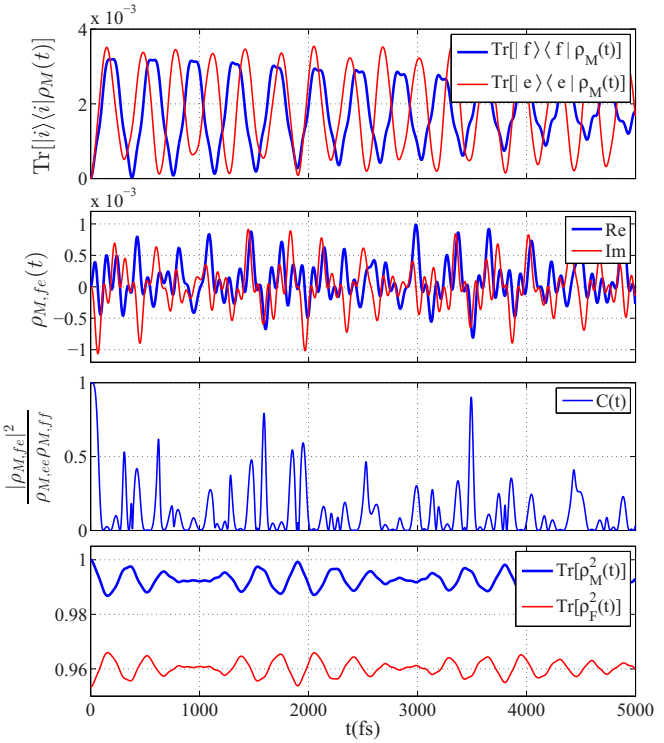

FIG. 8. From top to bottom: Excited-state populations ($|f\rangle$ state: blue thick line; $|e\rangle$ state: red thin line), coherence element (real: blue thick line; imaginary: red thin line), coherence measure, and partial traces (material: blue thick line; field: red thin line) obtained for the V system interacting with the three-mode thermal state, initially with $\bar{n}_k \ll 1$ and $\frac{\Delta_{i,k}}{\lambda_{i,k}} > 1$.

In this context, it is interesting to recall another example where single-mode thermal states bring about a dynamical pattern with well-separated collapses and revivals rather than the familiar chaotic one [17]. In that case, a single-mode thermal state interacts with N two-level systems and the interpretation is that the thermal state acquires attributes of coherent behavior due to the interaction with many equivalent two-level systems initially in the simplest possible initial state.

To conclude this section, we note that it is evident that the large similarity obtained for the thermal- and coherent-state-induced dynamics with initially $\bar{n} \ll 1$ is due to the fact that the two fields have almost the same photon number distribution, populating mainly the vacuum state. By considering $\bar{n} \gg 1$ and the distinct influence of the ratio $\frac{\Delta_i}{\lambda_i}$, it is evident that the single-mode thermal state, even though first-order coherent, differs from a coherent state. Nevertheless, both states induce excited-state (material) coherence. Last, we note that the effect of detuning was considered for a two-level system interacting with a coherent state [41,42] and numerically analyzed for a three-level system interacting with two modes [7] and with a single coherent mode [9]. In the two latter cases, the dynamical patterns for various parameters are calculated. In this context, the fact that the ratio $\frac{\Delta_i}{\lambda i}$ has a significant influence on the thermal-light-induced dynamics, as we have shown above, suggests that a more detailed study on the influence of detuning may be of interest.

B. V-type system interacting with three-mode thermal field

At this point we proceed to examine the interaction of a three-mode thermal state with the V-type three-level system, following the theoretical formulation of Eq. (1). We are particularly interested in the characteristics of the induced material coherence. This time we focus on the low average-photon-number limit, as it is relevant for sunlight. We also restrict ourselves to the $\frac{\Delta_i}{\lambda_i} > 1$ case since we would like detuning to play a role. Concretely, the initial average photon numbers of the three thermal modes are $\bar{n}_1 = 0.008\,5$, $\bar{n}_2 = 0.008$, and $\bar{n}_3 = 0.007\,6$, and the interaction constants are $\lambda_{i,1} = 1.5 \times 10^{-4}$, $\lambda_{i,2} = 10^{-4}$, and $\lambda_{i,3} = 9.5 \times 10^{-5}$. The mode detunings are $\Delta_{e,1} = \Delta_{f,2} = 3.80 \times 10^{-4}$ and $\Delta_{f,3} = -3.80 \times 10^{-4}$.

In Fig. 8 we show, from top to bottom, the excited-state material populations, material excited-state coherence element, coherence measure C(t), and traces of the material and field squared reduced density matrices obtained for the three-mode thermal state interacting with the V system. Clearly, the dynamical pattern is far more complex than that obtained for the single-mode thermal state, shown in Fig. 3. The three-mode thermal state does induce excited-state coherence with an apparent irregular revivals pattern of C(t) along the interaction period. We should note that, here too, the three modes remain completely diagonal in the course of interaction. In Fig. 9, we show the dynamical measures obtained for the same matter-field configuration but the initial field is a coherent

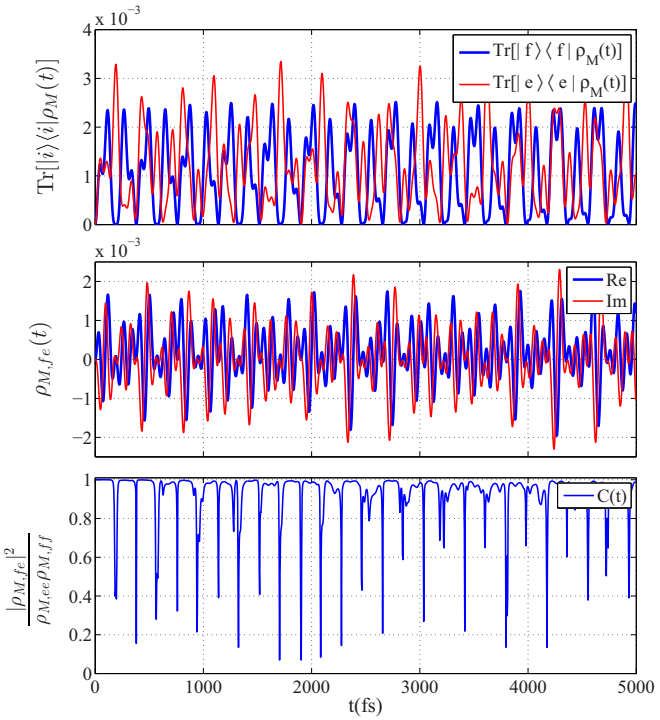

FIG. 9. From top to bottom: Excited-state populations ($|f\rangle$ state: blue thick line; $|e\rangle$ state: red thin line), coherence element (real: blue thick line; imaginary: red thin line), coherence measure obtained for the V system interacting with a three-mode coherent state, initially with $\bar{n}_k \ll 1$ and $\frac{\Delta_{i,k}}{\lambda_{i,k}} > 1$.

state. Both figures indicate a complex time dependence that apparently depends on the multimode detunings. We note, although we do not show here, that two-mode thermal state of the field induces excited-state material coherence as well. To fully characterize the interaction of multimode with the material system, further study is required. In particular, the $\bar{n} \gg 1$ and $\frac{\Delta_i}{\lambda_i} \ll 1$ regimes should be considered as well but are beyond the scope of the current work.

Within a fully quantum-mechanical dynamical framework, the ultimate model for the interaction of sunlight with matter would probably consist of a continuous-mode description [40] of the light. Previous works have employed a number of limited models for studying the interaction of thermal light with matter, for example, [26,27], where the common conclusion was that thermal light could not induce excited-state coherence and the state of the material system would be a mixture of eigenstates. In contrast, our results for single- and three-mode thermal states show that this kind of thermal light does indeed induce coherence in the material excited states. Indeed, the thermal states do not induce coherence between the ground and excited states, and thus the material system is a mixture of a ground state and a superposition of the excited states. For a more complete picture of the interaction of the V system with thermal light, the generalization to an arbitrary number of modes is required, but our results do not indicate any fundamental restriction for coherence to be induced.

TABLE I. The parameters, in atomic units, for PESs used for the molecular simulations.

	V_g	V_e
D	0.0378492	0.0426108
b	0.4730844	0.3175063
r_0	5.0493478	5.8713786
T	0	0.0911267

C. Two-state Born-Oppenheimer system interacting with single-mode thermal field

The motivation for studying the interaction of thermal light with the simplest multiple excited-state system—the V-type three-level system—is to develop some understanding for the case of a realistic molecular system. Such a system can consist of ground and excited electronic states, each with their manifold of vibrational levels. It can be expected that a direct analogy to the V system would apply.

We follow the theoretical framework presented above to test the JC molecular extension and thus simulate the interaction of a single-mode thermal state of the light with a two-state Born-Oppenheimer PES molecular system. In practice, we consider a molecular system of two one-dimensional Morse-type PESs, $V_i(\boldsymbol{r}) = D_i(1 - e^{-b_i(\boldsymbol{r}-r_{0i})})^2 + T_i$. The potential parameters we use for the simulation are specified in Table I; these are essentially the X and A states of the Li_2 molecule [43] used in a previous study [44], but only with the A state (V_e in the notation used here) shifted in energy.

The initial state of the field $\rho_F(0) = \sum_n p_n|n\rangle\langle n|$ is constructed with the first seven Fock states. We set $\lambda = 10^{-4}$, and $\bar{n} = 0.007\,2$ (obtained for 486.1 nm at 6000 K for the field mode). The molecular subsystem is represented in coordinate space and the thermal mode can "naturally" couple the molecular ground state with the infinite set of excited vibrational states. Note that the vibrational ground state (of the $|g\rangle$ electronic state) has different overlap with each of the vibrational excited states (of the $|e\rangle$ electronic state). Therefore, although we use a single value for λ, the field mode couples the vibrational ground state to each of the vibrational excited states with different effective strengths. The frequency of the excited mode is tuned between the third and fourth vibrational eigenstates of the excited state $|e\rangle$. This configuration is analogous to the detuned case considered above for the V system, whose results are presented in Fig. 3. Based on these results for the interaction of the single-mode thermal state with the V system, we can expect the thermal light to induce molecular excited-state coherence.

In Fig. 10 we show snapshots of the excited-state material reduced density matrix, $\rho_{M,ee}(t)$. In the left column we show $\rho_{M,ee}(t)$ in the coordinate representation, while in the right column we show its projection onto the first 15 excited vibrational eigenstates. The clear observation that emerges from these snapshots is that thermal light induces excited-state vibrational coherence (dominated by the third and fourth vibrational states) that persists for several vibration periods. An almost identical coherence feature is obtained by the interaction of a coherent state with the molecular system (not shown here), as we can expect on the basis of the

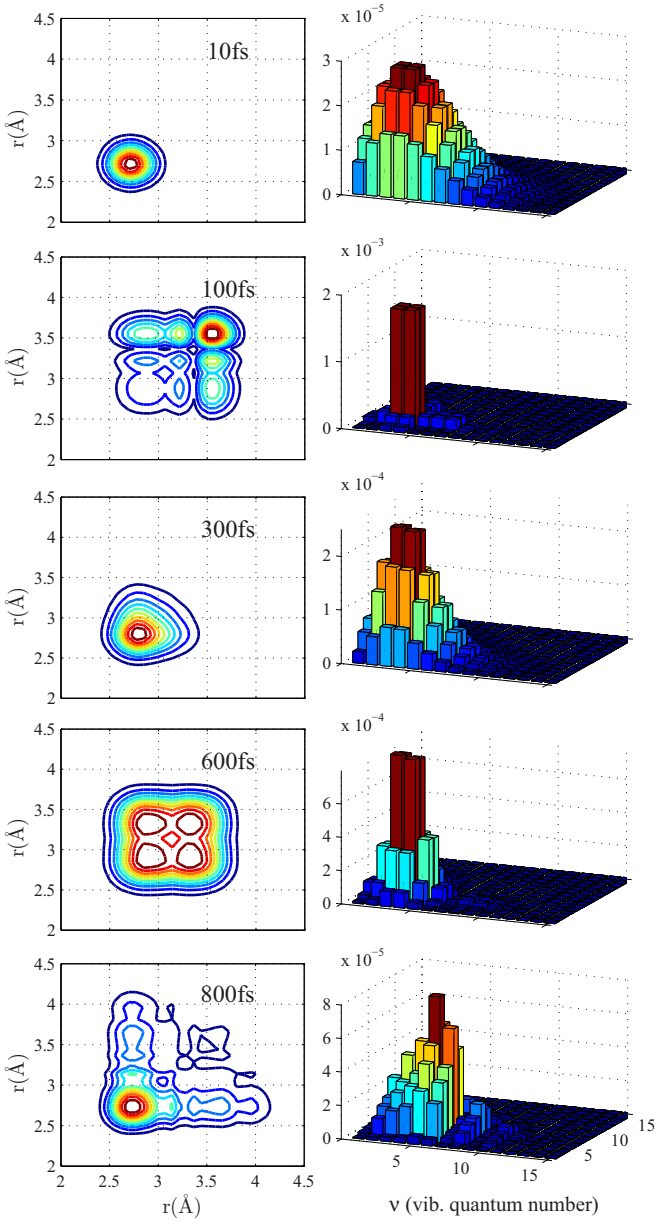

FIG. 10. Snapshots of $\rho_{M,ee}(t)$ for thermal light interacting with a two-state Born-Oppenheimer molecule. The left column shows $\rho_{M,ee}(t)$ in coordinate space (with the time specified in femtoseconds), and the right column shows its projection onto the vibrational eigenstates of the molecular excited state.

results obtained for the V system. The spatial representation exhibits a wave-packet-like dynamics, unlike that reported on the basis of a semiclassical treatment with pulsed incoherent light [35]. It is interesting to note, although we do not show it here, that when the field is resonant with a vibrational eigenstate of the excited state, the wave packet created initially evolves to the corresponding vibrational eigenstates within a single vibrational cycle on the excited state. This applies to the coherent and thermal states. The difference between the interaction with coherent and thermal states is that the former also induces coherence between the ground and excited electronic states while the latter does not, just as discussed

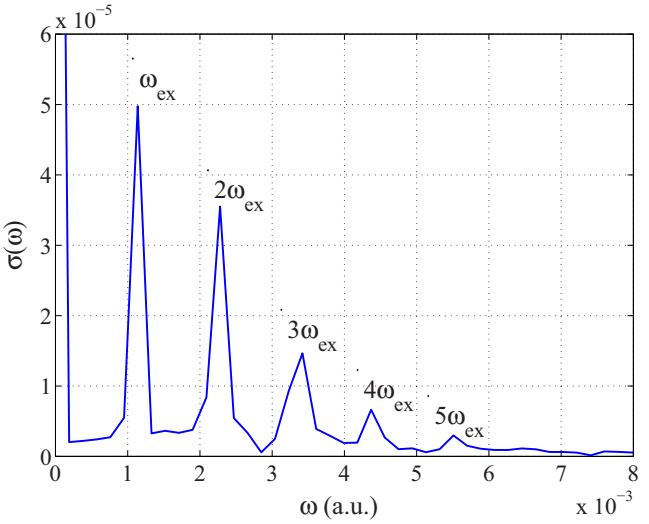

FIG. 11. The spectrum obtained by Fourier transform of the excited-state molecular autocorrelation function $\mathcal{C}(t) = \mathrm{Tr}[\rho_{M,gg}(0)\rho_{M,ee}(t)]$.

above for the V system. To have a quantitative measure of the wave-packet-like dynamics, we calculate the excited-state correlation function $\mathcal{C}(t) = \mathrm{Tr}[\rho_{M,gg}(0)\rho_{M,ee}(t)]$ and its Fourier transform $\sigma(\omega)$. In Fig. 11 we show the spectrum $\sigma(\omega)$. It reveals the harmonics of the characteristic energy difference between the excited-state vibrational eigenstates $\omega_{ex} \approx 0.0011$ a.u.

The dynamical picture obtained for the case where the initial average photon number of the field is $\bar{n} = 3$ (not shown here) is quite similar to that seen in Fig. 10, and the typical chaotic pattern becomes pronounced as the interaction constant becomes relatively large. This is in agreement with the results for the V system.

The results for the single-mode-induced dynamics may well represent a molecule (or an atom, in the case of the V system) residing in a cavity and interacting with the electromagnetic mode. It is important in this context to note that all of the attempts to model the interaction of quantized thermal light with matter, that were mentioned in the Introduction, have actually employed cavity dynamics as well. A more realistic model, for the interaction of sunlight with matter, demands a continuous-mode formalism [40], or, at least, a multimode formulation. Based on the thermal three-mode results above for the V system, we believe that in the relevant photon number regime, that is $\bar{n} \ll 1$, a multimode thermal light would induce excited-state coherence in the molecular system as well. It may also be of interest to examine the influence on the initial state of the molecular system on the subsequent dynamics. Particularly, the possibility that the molecule is initially in a mixed state of the ground vibrational states is most relevant for systems at high temperature.

IV. CONCLUSIONS

Thermal-light-induced dynamics of molecular systems is of great interest. A number of methodologies have been applied to study thermal-light-induced dynamics of material systems but

have not provided a consistent conclusion regarding induced material coherence. Furthermore, semiclassical and fully quantized methodologies for thermal-light-induced dynamics in two-level systems have indicated different dynamical characteristics. In this context, a fully quantized framework for studying the interaction of realistic molecular systems with thermal light is necessary to understand the corresponding dynamics.

In light of this, we study the interaction of a quantized thermal state of the electromagnetic field with matter, with a focus on two main aspects that have not been considered before. The first relates to the question of whether a thermal state, and in particular, a multimode thermal state, induces material coherence. In the second, we extend the Jaynes-Cummings (JC) model to a molecular system of two-state Born-Oppenheimer potential energy surface (PES) where the vibrational degrees of freedom are taken into account. We are mostly interested in the low-average-photon-number regime, $\bar{n} \ll 1$, as it is relevant to the much-studied topic of sunlight-induced chemical reactions in natural photosynthetic systems.

By employing a JC-type interaction model for a V-type three-level system and multimode thermal state of the light, it is shown that the thermal light does induce excited-state coherence in the material subsystem, contrary to previously stated conclusions. Indeed, the thermal state, which remains diagonal throughout the dynamics, does not induce coherence between the material ground state and the excited states. In addition, we show that the ratio of field detuning and interaction constant has a significant influence on the thermal-light-induced dynamics. In particular, in some circumstances, thermal light can bring about dynamical time dependence that shows a "coherentlike" collapse-and-revival pattern rather than the characteristic chaotic pattern. Such an effect has been reported before for single-mode thermal light interacting with many two-level systems.

We further extend the JC model for a molecular system that consists of two-state Born-Oppenheimer PESs, where the light-matter system is represented, and propagated, in the electronic–bond-coordinate–Fock product space using a density-matrix formalism. We show that a single-mode thermal state of the field induces extensive vibrational coherence in the molecular excited state that is manifested by wave-packet-like dynamics in the material coordinate space. On the basis of the results obtained for the V system interacting with a thermal multimode field, we expect that a similar excited-state vibrational coherence would be induced by a thermal multimode field.

Our results suggest that it should be worthwhile to reconsider the previous general conclusion, drawn in earlier studies, that thermal light should induce only a mixture of material eigenstates. In particular, our results do not indicate any fundamental restriction for excited-state coherence to be induced by thermal light. The generalization of the fully quantized treatment to an arbitrary number of modes, and to continuous mode, is expected to remove any existing ambiguity in this issue. For a complete understanding of the nature of the interaction of thermal light with atomic and molecular systems, the effects of detuning and initial state of the material systems should be further studied as well. Last, the molecular JC model we propose may be used for cavity molecular dynamics simulations.

APPENDIX: ANALYTICAL DYNAMICAL EXPRESSIONS FOR THE V-TYPE THREE-LEVEL SYSTEM

In this section, we derive analytical expressions for the populations and coherence of the V-type three-level subsystem for the case where the single-mode frequency is equally (and oppositely) detuned from the excited states. In other words, the excited states are not degenerate and $\Delta = \omega_f - \omega = -(\omega_e - \omega)$. In addition, we set the interaction constants equal, denoted by λ. Following [2], the interaction Hamiltonian for the case we consider here is thus given in the material states basis by

$$H_I = \begin{pmatrix} \Delta & 0 & \lambda\hat{a} \\ 0 & -\Delta & \lambda\hat{a} \\ \lambda\hat{a}^\dagger & \lambda\hat{a}^\dagger & 0 \end{pmatrix}. \tag{A1}$$

Employing a Taylor expansion, the corresponding propagator is given by

$$e^{-iH_I t} = \begin{pmatrix} \hat{C}_{ff} - i\hat{S}_{ff} & \hat{C}_{fe} & \hat{C}_{fg} - i\hat{S}_{fg} \\ \hat{C}_{fe} & \hat{C}_{ff} + i\hat{S}_{ff} & -\hat{C}_{fg} - i\hat{S}_{fg} \\ \hat{C}_{gf} - i\hat{S}_{gf} & -\hat{C}_{gf} - i\hat{S}_{gf} & \hat{C}_{gg} \end{pmatrix}, \tag{A2}$$

with the Fock-space operators given by

$$\begin{aligned}
\hat{C}_{ff} &= \frac{1}{\Omega}\left[\cos(\sqrt{\Omega}t) + \left(\frac{\Omega}{\Theta} - 1\right)\right]\Theta \\
\hat{S}_{ff} &= \frac{\Delta}{\sqrt{\Omega}}\sin(\sqrt{\Omega}t) \\
\hat{C}_{fe} &= \frac{\lambda^2}{\Omega}[\cos(\sqrt{\Omega}t) - 1]\hat{a}\hat{a}^\dagger \\
\hat{C}_{fg} &= \frac{\lambda\Delta}{\Omega}[\cos(\sqrt{\Omega}t) - 1]\hat{a} \\
\hat{S}_{fg} &= \frac{\lambda}{\sqrt{\Omega}}\sin(\sqrt{\Omega}t)\hat{a} \\
\hat{C}_{gf} &= \frac{\lambda\Delta}{\widetilde{\Omega}}[\cos(\sqrt{\widetilde{\Omega}}t) - 1]\hat{a}^\dagger \\
\hat{S}_{gf} &= \frac{\lambda}{\sqrt{\widetilde{\Omega}}}\sin(\sqrt{\widetilde{\Omega}}t)\hat{a}^\dagger \\
\hat{C}_{gg} &= \frac{2\lambda^2}{\widetilde{\Omega}}\left[\cos(\sqrt{\widetilde{\Omega}}t) + \left(\frac{\widetilde{\Omega}}{2\lambda^2\hat{a}^\dagger\hat{a}} - 1\right)\right]\hat{a}^\dagger\hat{a},
\end{aligned} \tag{A3}$$

where we define $\Omega \equiv \Delta^2 + 2\lambda^2\hat{a}\hat{a}^\dagger$, $\widetilde{\Omega} \equiv \Delta^2 + 2\lambda^2\hat{a}^\dagger\hat{a}$, and $\Theta \equiv \Delta^2 + \lambda^2\hat{a}\hat{a}^\dagger$. The operation of each operator on the Fock basis states is then

$$\begin{aligned}
\hat{C}_{ff}|n\rangle &= \frac{1}{\Omega_{n+1}}\left[\cos(\sqrt{\Omega_{n+1}}t) + \left(\frac{\Omega_{n+1}}{\Theta_{n+1}} - 1\right)\right]\Theta_{n+1}|n\rangle \\
\hat{S}_{ff}|n\rangle &= \frac{\Delta}{\sqrt{\Omega_{n+1}}}\sin(\sqrt{\Omega_{n+1}}t)|n\rangle \\
\hat{C}_{fe}|n\rangle &= \frac{\lambda^2}{\Omega_{n+1}}[\cos(\sqrt{\Omega_{n+1}}t) - 1]|n\rangle
\end{aligned}$$

$$\begin{aligned}
\hat{C}_{fg}|n\rangle &= \frac{\lambda\Delta}{\Omega_n}[\cos(\sqrt{\Omega_n}t)-1]\sqrt{n}|n-1\rangle \\
\hat{S}_{fg}|n\rangle &= \frac{\lambda}{\sqrt{\Omega_n}}\sin(\sqrt{\Omega_n}t)\sqrt{n}|n-1\rangle \\
\hat{C}_{gf}|n\rangle &= \frac{\lambda\Delta}{\Omega_{n+1}}[\cos(\sqrt{\Omega_{n+1}}t)-1]\sqrt{n+1}|n+1\rangle \\
\hat{S}_{gf}|n\rangle &= \frac{\lambda}{\sqrt{\Omega_{n+1}}}\sin(\sqrt{\Omega_{n+1}}t)\sqrt{n+1}|n+1\rangle \\
\hat{C}_{gg}|n\rangle &= \frac{2\lambda^2}{\Omega_n}\left[\cos(\sqrt{\Omega_n}t)+\left(\frac{\Omega_n}{2\lambda^2 n}-1\right)\right]n|n\rangle,
\end{aligned} \tag{A4}$$

where we define $\Omega_n \equiv \Delta^2 + 2\lambda^2 n$ and $\Theta_n \equiv \Delta^2 + \lambda^2 n$.

Assuming the material subsystem is initially in its ground state and the general initial state $\rho_F(0)$ for the field subsystem, the initial state of the bipartite system $\rho_I(0)$ is given in the material states representation by

$$\rho_I(0) = \begin{pmatrix} 0 & 0 & 0 \\ 0 & 0 & 0 \\ 0 & 0 & \rho_F(0) \end{pmatrix}. \tag{A5}$$

Using the propagator defined in Eq. (A2) and its Hermitian conjugate, the system state at any time t is obtained by using the relation

$$\rho_I(t) = e^{-iH_I t}\rho_I(0)e^{iH_I t}. \tag{A6}$$

Specifically, for an initial thermal single mode of the field $\rho_F(0) = \sum_n p_n|n\rangle\langle n|$, the material excited-state populations are

$$\begin{aligned}
\rho_{M,ff}(t) &= \rho_{M,ee}(t) \\
&= (\lambda\Delta)^2\sum_n p_n\frac{n}{\Omega_n^2}[\cos(\sqrt{\Omega_n}t)-1]^2 \\
&\quad +\lambda^2\sum_n p_n\frac{n}{\Omega_n}\sin^2(\sqrt{\Omega_n}t).
\end{aligned} \tag{A7}$$

The material ground-state population is given by

$$\rho_{M,gg}(t) = \sum_n p_n\frac{(2\lambda^2 n)^2}{\Omega_n^2}\left[\cos(\sqrt{\Omega_n}t)+\frac{\Delta^2}{2\lambda^2 n}\right]^2, \tag{A8}$$

and the excited-state material coherence by

$$\begin{aligned}
&\rho_{M,fe}(t) = \\
&\lambda^2\sum_n p_n\frac{n}{\Omega_n}\left\{\sin^2(\sqrt{\Omega_n}t)-\frac{\Delta^2}{\Omega_n}[\cos(\sqrt{\Omega_n}t)-1]^2\right\} \\
&+2i\lambda^2\Delta\sum_n p_n\frac{n}{\Omega_n^{3/2}}\sin(\sqrt{\Omega_n}t)[\cos(\sqrt{\Omega_n}t)-1].
\end{aligned} \tag{A9}$$

Our simulations for the relevant physical case (not shown) fit to these analytical expressions.

It is easily verified, using the above analytical expressions with some algebra, that (1) the thermal mode remains diagonal throughout the dynamics, and (2) the ground excited-state material coherence element is identically zero at all times.

We now write approximate expressions for the material populations and coherence for the cases $\bar{n} \ll 1$ and $\bar{n} \gg 1$. We also specify the expressions for different $\frac{\Delta}{\lambda}$ ratios. We begin with $\bar{n} \ll 1$. In this case, the thermal distribution coefficients are approximately $p_n \approx \bar{n}^n$. We thus get for the populations and coherences the following expressions:

$$\begin{aligned}
\rho_{M,ff}^{\bar{n}\ll 1}(t) &\approx (\lambda\Delta)^2\sum_n\frac{\bar{n}^n n}{\Omega_n^2}[\cos(\sqrt{\Omega_n}t)-1]^2 \\
&\quad +\lambda^2\sum_n\frac{\bar{n}^n n}{\Omega_n}\sin^2(\sqrt{\Omega_n}t),
\end{aligned} \tag{A10}$$

and

$$\begin{aligned}
&\rho_{M,fe}^{\bar{n}\ll 1}(t) \approx \\
&\lambda^2\sum_n\frac{\bar{n}^n n}{\Omega_n}\left\{\sin^2(\sqrt{\Omega_n}t)-\frac{\Delta^2}{\Omega_n}[\cos(\sqrt{\Omega_n}t)-1]^2\right\} \\
&+2i\lambda^2\Delta\sum_n\frac{\bar{n}^n n}{\Omega_n^{3/2}}\sin(\sqrt{\Omega_n}t)[\cos(\sqrt{\Omega_n}t)-1].
\end{aligned} \tag{A11}$$

For the relatively large detuning regime, $\frac{\Delta}{\lambda} \gg 1$, these expressions are further approximated as

$$\rho_{M,ff}^{\bar{n}\ll 1,\frac{\Delta}{\lambda}\gg 1}(t) \approx \left(\frac{2\lambda}{\Delta}\right)^2\sin^2\left(\frac{\Delta}{2}t\right)\sum_n\bar{n}^n n \tag{A12}$$

and

$$\rho_{M,fe}^{\bar{n}\ll 1,\frac{\Delta}{\lambda}\gg 1}(t) \approx \left(\frac{2\lambda}{\Delta}\right)^2 e^{-i\Delta t}\sin^2\left(\frac{\Delta}{2}t\right)\sum_n\bar{n}^n n. \tag{A13}$$

We now turn to the $\bar{n} \gg 1$ case, where the thermal state initial distribution coefficients are, approximately, $p_n \approx \bar{n}^{-1}$. The excited-state population and coherence terms now take the approximate forms of

$$\begin{aligned}
\rho_{M,ff}^{\bar{n}\gg 1}(t) &\approx (\lambda\Delta)^2\sum_n\frac{\bar{n}^{-1} n}{\Omega_n^2}[\cos(\sqrt{\Omega_n}t)-1]^2 \\
&\quad +\lambda^2\sum_n\frac{\bar{n}^{-1} n}{\Omega_n}\sin^2(\sqrt{\Omega_n}t),
\end{aligned} \tag{A14}$$

and

$$\begin{aligned}
&\rho_{M,fe}^{\bar{n}\gg 1}(t) \\
&\approx \lambda^2\sum_n\frac{\bar{n}^{-1} n}{\Omega_n}\left\{\sin^2(\sqrt{\Omega_n}t)-\frac{\Delta^2}{\Omega_n}[\cos(\sqrt{\Omega_n}t)-1]^2\right\} \\
&\quad +2i\lambda^2\Delta\sum_n\frac{\bar{n}^{-1} n}{\Omega_n^{3/2}}\sin(\sqrt{\Omega_n}t)[\cos(\sqrt{\Omega_n}t)-1].
\end{aligned} \tag{A15}$$

For a relatively small detuning $\frac{\Delta}{\lambda} \ll 1$, we then have

$$\rho_{M,ff}^{\bar{n}\gg 1,\frac{\Delta}{\lambda}\ll 1}(t) = \rho_{M,fe}^{\bar{n}\gg 1,\frac{\Delta}{\lambda}\ll 1}(t) \approx \frac{1}{2\bar{n}}\sum_n\sin^2(\sqrt{2n}\lambda t). \tag{A16}$$

[1] E. T. Jaynes and F. W. Cummings, Proc. IEEE **51**, 89 (1963).
[2] H.-I. Yoo and J. H. Eberly, Phys. Rep. **118**, 239 (1985).
[3] B. W. Shore and P. L. Knight, J. Mod. Opt. **40**, 1195 (1993).
[4] E. G. Groves, B. D. Clader, and J. H. Eberly, J. Phys. B: At., Mol. Opt. Phys. **46**, 224005 (2013).
[5] M. Tavis and F. Cummings, J. Phys. B: At., Mol. Opt. Phys. **46**, 224011 (2013).
[6] S. Stenholm, J. Phys. B: At., Mol. Opt. Phys. **46**, 224013 (2013).
[7] X.-S. Li and Y.-N. Peng, Phys. Rev. A **32**, 1501 (1985).
[8] A.-S. Obada and A. M. Abdal-Hafez, J. Mod. Opt. **34**, 665 (1987).
[9] X.-S. Li, D. L. Lin, and C.-D. Gong, Phys. Rev. A **36**, 5209 (1987).
[10] D. A. Cardimona, M. P. Sharma, and M. A. Ortega, J. Phys. B: At., Mol. Opt. Phys. **22**, 4029 (1989).
[11] F. W. Cummings, Phys. Rev. **140**, A1051 (1965).
[12] P. L. Knight and P. M. Radmore, Phys. Lett. A **90**, 342 (1982).
[13] G. Arroyo-Correa and J. J. Sanchez-Mondragon, Quantum Opt. **2**, 409 (1990).
[14] M. Kozierowski, S. M. Chumakov, and J. J. Sanchez-Mondragon, J. Mod. Opt. **40**, 1763 (1993).
[15] C. A. Aranciba, S. M. Chumakov, and J. J. Sanchez-Mondragon, J. Mod. Opt. **40**, 2071 (1993).
[16] S. M. Chumakov, M. Kozierowski, and J. J. Sanchez-Mondragon, Phys. Rev. A **48**, 4594 (1993).
[17] S. M. Chumakov and J. J. Sanchez-Mondragon, Opt. Commun. **107**, 231 (1994).
[18] R. W. Schoenlein, L. A. Peteanu, R. A. Mathies, and C. V. Shank, Science **254**, 412 (1991).
[19] M. H. Vos, J.-C. Lambry, S. J. Robles, D. C. Youvan, J. Breton and J.-L. Martin, Proc. Natl. Acad. Sci. USA **88**, 8885 (1991).
[20] S. L. Dexheimer, Q. Wang, L. A. Peteanu, W. T. Pollard, R. A. Mathies, and C. V. Shank, Chem. Phys. Lett. **188**, 61 (1992).
[21] Q. Wang, R. W. Schoenlein, L. A. Peteanu, R. A. Mathies, and C. V. Shank, Science **266**, 422 (1994).
[22] G. S. Engel, T. R. Chalhoun, E. L. Read, T.-K. Ahn, T. Mančal, Y.-C. Cheng, R. E. Blankenship, and G. R. Fleming, Nature (London) **446**, 782 (2007).
[23] H. Lee, Y.-C. Cheng, and G. R. Fleming, Science **316**, 1462 (2007).
[24] G. Panitchayangkoon, D. Hayes, K. A. Fransted, J. R. Caram, E. Harel, J. Wen, R. R. Blankenship, and G. S. Engel, Proc. Natl. Acad. Sci. USA **107**, 12766 (2010).
[25] E. Collini, C. Y. Wong, K. E. Wilk, P. M. G. Curmi, P. Brumer, and G. D. Scholes, Nature (London) **463**, 644 (2010).
[26] P. Brumer and M. Shapiro, Proc. Natl. Acad. Sci. USA **109**, 19575 (2012).
[27] X.-P. Jiang and P. Brumer, J. Chem. Phys. **94**, 5833 (1991).
[28] M. Fleischhauer, C. H. Keitel, M. O. Scully, and C. Su, Opt. Commun. **87**, 109 (1992).
[29] G. C. Hegerfeldt and M. B. Plenio, Phys. Rev. A **47**, 2186 (1993).
[30] V. V. Kozlov, Y. Rostovtsev, and M. O. Scully, Phys. Rev. A **74**, 063829 (2006).
[31] K. E. Dorfman, D. V. Voronine, S. Mukamel, and M. O. Scully, Proc. Natl. Acad. Sci. USA **110**, 2746 (2013).
[32] T. V. Tscherbul and P. Brumer, Phys. Rev. Lett. **113**, 113601 (2014).
[33] D. Bortman-Arbiv, A. D. Wilson-Gordon, and H. Friedmann, Phys. Rev. A **63**, 043818 (2001).
[34] A. W. Chin, J. Prior, R. Rosenbach, F. Caycedo-Soler, S. F. Huelga, and M. B. Plenio, Nat. Phys. **9**, 113 (2013).
[35] A. C. Han, M. Shapiro, and P. Brumer, J. Phys. Chem. A **117**, 8199 (2013).
[36] Z. S. Sadeq and P. Brumer, J. Chem. Phys. **140**, 074104 (2014).
[37] C. Gerry and P. Knight, *Introductory Quantum Optics* (Cambridge University Press, Cambridge, UK, 2005).
[38] D. J. Tannor, *Introduction to Quantum Mechanics: A Time-Dependent Perspective* (University Science Books, Sausalito, CA, 2007).
[39] G. J. Milburn, Opt. Acta **31**, 671 (1984).
[40] R. Loudon, *The Quantum Theory of Light*, 3rd ed. (Oxford University Press, Oxford, UK, 2000).
[41] S. Stenholm, Phys. Rep. **6**, 1 (1973).
[42] M. Hillery and R. J. Schwartz, Phys. Rev. A **43**, 1506 (1991).
[43] G. Herzberg, in *Molecular Spectra and Molecular Structures, I. Spectra of Diatomic Molecules* (Krieger Publishing Company, Malabar, FL, 1950).
[44] D. Avisar and D. J. Tannor, Phys. Rev. Lett. **106**, 170405 (2011).